Electrochemistry Communications 113 (2020) 106689

Contents lists available at ScienceDirect

Electrochemistry Communications

journal homepage: www.elsevier.com/locate/elecom

Full Communication

Redox and optically active carbohelicene layers prepared by potentiodynamic polymerization

Jan Hrbac[a], Vit Pavelka[a], Jeanne Crassous[b], Jaroslav Zadny[c], Ladislav Fekete[d], Jan Pokorny[d], Petr Vanysek[e], Jan Storch[c,*], Jan Vacek[f,*]

[a] Institute of Chemistry, Masaryk University, Kamenice 5, 725 00 Brno, Czech Republic
[b] Univ Rennes, Institut des Sciences Chimiques de Rennes, CNRS UMR 6226, Campus de Beaulieu, Rennes Cedex, France
[c] Institute of Chemical Process Fundamentals, Czech Academy of Sciences, Rozvojova 135, 165 02 Prague 6, Czech Republic
[d] Institute of Physics of the Czech Academy of Sciences, Na Slovance 2, Prague, Czech Republic
[e] Department of Electrical and Electronic Technology, Faculty of Electrical Engineering and Communication, Brno University of Technology, Technická 3058/10, 616 00 Brno, Czech Republic
[f] Department of Medical Chemistry and Biochemistry, Faculty of Medicine and Dentistry, Palacky University, Hnevotinska 3, 775 15 Olomouc, Czech Republic

ARTICLE INFO

Keywords:
Carbohelicene
Hexahelicene
Voltammetry
Enantiopure
Redox active
Chiral carbon

ABSTRACT

This short paper describes the preparation of thin layers based on carbohelicenes, which are inherently chiral polyaromatics existing in the enantiomeric forms P and M. Specifically, [5]-, [6]- and [7]helicene were subjected to redox cycling between −1.5 and 1.5 V *vs.* ferrocene/ferrocenium at a scan rate of 10 V/s. This way, enantiopure layers exhibiting redox activity were formed on the surfaces of the glassy carbon and ITO electrodes under anoxic and non-aqueous conditions. The properties of the prepared polymer layers were investigated using electrochemistry with Fe/Ru redox probes, circular dischroism, AFM, impedance measurement and Raman spectroscopy. With [6]helicene, the suggested electropolymerization procedure thus represents a proof-of-concept for the preparation of chiral carbonaceous surfaces.

1. Introduction

Helicenes, with their non-planar inherently chiral topology, semiconductivity and unique non-linear optical properties, represent a class of compounds with extremely high application potential. One promising area for their utilization is the sensing of chiral molecules due to their ability to enantiodiscriminate [1–5]. The simple fabrication of a helicene layer by various solution coating techniques or anodic deposition enables the easy construction of thin-film devices, *e.g.* OLEDs [6], a humidity sensor etc. With helicenes, anodic deposition is a powerful tool for the creation of new polymeric materials with the advantage of no need for the previous functionalization of the starting monomers. In our previous study [7], we showed that electrosynthesis is a useful tool for the preparation of chiral [6]helicene-based layers, however the protocol used led to non-conductive thin films. Here we describe for the first time the synthesis of redox-active carbohelicene-based enantiopure layers, although only the reduced form is fully stable. The results indicate that carbohelicenes are electropolymerizable species capable of producing both electroactive and insulating polymers, directly analogous to conductive and overoxidized versions of *e.g.* polypyrrole or polythiophene.

2. Experimental

2.1. Reagents

The racemic [5]-, [6]- and [7]helicene were synthesized according to our previous study [7] and its references. Acetonitrile (HPLC grade), tetrabutylammonium perchlorate (TBAP, for electrochemistry) and hexaammineruthenium (III) chloride were from Sigma-Aldrich. Potassium chloride and potassium hexacyanoferrate (III) were from Lachema Brno, CZ; ferrocene was purchased from Fluka.

2.2. Resolution of [6]helicene

The resolution of [6]helicene enantiomers was performed by preparative HPLC with a UV detector according to the published procedures [8,9].

* Corresponding authors.
E-mail addresses: storchj@icpf.cas.cz (J. Storch), jan.vacek@upol.cz (J. Vacek).

https://doi.org/10.1016/j.elecom.2020.106689
Received 13 February 2020; Accepted 13 February 2020
Available online 19 February 2020

2.3. Electrochemistry

Electrochemical experiments were carried out using Nanoampere2 workstation (L-Chem, CZ) in three-electrode configuration. A GC electrode (3 mm dia, CHI104, CH Instruments, USA), indium tin oxide-coated glass slide (surface resistivity 8–12 Ω/sq., Sigma-Aldrich, cat. No. 703192) or indium tin oxide-coated PET (surface resistivity 60 Ω/sq., Sigma-Aldrich, cat. No. 639303) were used as working electrodes, and a platinum plate served as the auxiliary electrode. For non-aqueous electrochemistry, carried out in 0.1 M TBAP dissolved in acetonitrile, a silver rod (purity 99.95%, diameter 2 mm, Alfa Aesar, Germany) served as a pseudo-reference electrode. Under these conditions, the midpoint potential of ferrocene determined by cyclic voltammetry was 438 mV. The potential scales of nonaqueous voltammetric experiments were referenced to ferrocene/ferrocenium redox potential by subtracting the above figure from voltammetric X-data. An Ag/AgCl, 3 M KCl reference electrode (CHI 111, CH Instruments, U.S.A.) was used for electrochemical experiments in aqueous environments. eL-ChemViewer 2.0 freeware [10] was used for voltammetric data post processing. Where appropriate, the solutions were deoxygenated by argon purging. The electrochemical impedance spectra were recorded using Ametek ModuLab XM ECS instrument.

2.4. Raman spectroscopy

Unpolarized Raman spectra were collected using a Renishaw inVia Reflex (325 nm excitation) micro-Raman spectrometer, operating in a standard back-scattering configuration. The details on Raman spectra collection can be found in Ref. [7].

2.5. AFM imaging

The measurements were performed with an ambient Bruker Dimension Icon microscope. To visualize the morphology of the samples, soft cantilevers with a low spring constant, k = 0.4 Nm^{-1} were used (ScanAsyst air), with the resonant frequency in the range of 70–80 kHz at room temperature. The images were taken with a resolution of 512 × 512 points^2 in the PeakForce QNM type of measurement.

2.6. CD spectroscopy

Circular dichroism (CD) and UV–vis spectra were measured in a Jasco J-815 Circular Dichroism Spectrometer (IFR140 facility – Biosit – Université de Rennes 1).

3. Results and discussion

3.1. Experiments with GC electrode

The aim of this paper was to prepare enantiomerically pure thin films which are redox active. Unlike previously published approaches [11,12], the electrosynthetic approach described in this work utilizes unsubstituted helicenes, *i.e.* carbohelicenes. For this purpose, the racemic monomers [5]-, [6]- and [7]helicene were first used, these being equimolar mixtures of the respective P and M enantiomers. Anodic deposition onto the GC electrode from solutions of monomers in ACN containing 0.1 M TBAP was used to prepare the layers. The electrosynthesis is based on redox cycling in the potential range between –1.5 and 1.5 V *vs.* $Fc/Fc^{\cdot+}$. The anodic potential limit is the determining parameter; when exceeded, the overoxidation of the deposited layer results in the loss of redox activity or conductivity properties [12,13]. The layer growth is initiated by reactive cation radicals generated in the course of oxidation, causing monomer interlinkage leading to a covalently bound layer [7,12,13]. CV records obtained under anoxic conditions are shown in Fig. 1, which show that the current response at ca. +1.3 V decreases. The decline in CV peak corresponds to the formation of radical cations and with monomer depletion near the working electrode. In contrast, a gradual increase in current at approx. +0.8 V occurs during repeated CV scans, provided that sufficiently fast scan rates are used. Simultaneously with the increase in anodic currents, an increase in the cathodic region can be observed as well, fully corresponding to the formation of a redox-active film. The formation of this redox-active film occurs under anoxic conditions, *cf.* Figs. 1 and S1 in the Supporting Information. The requirement of relatively high scan

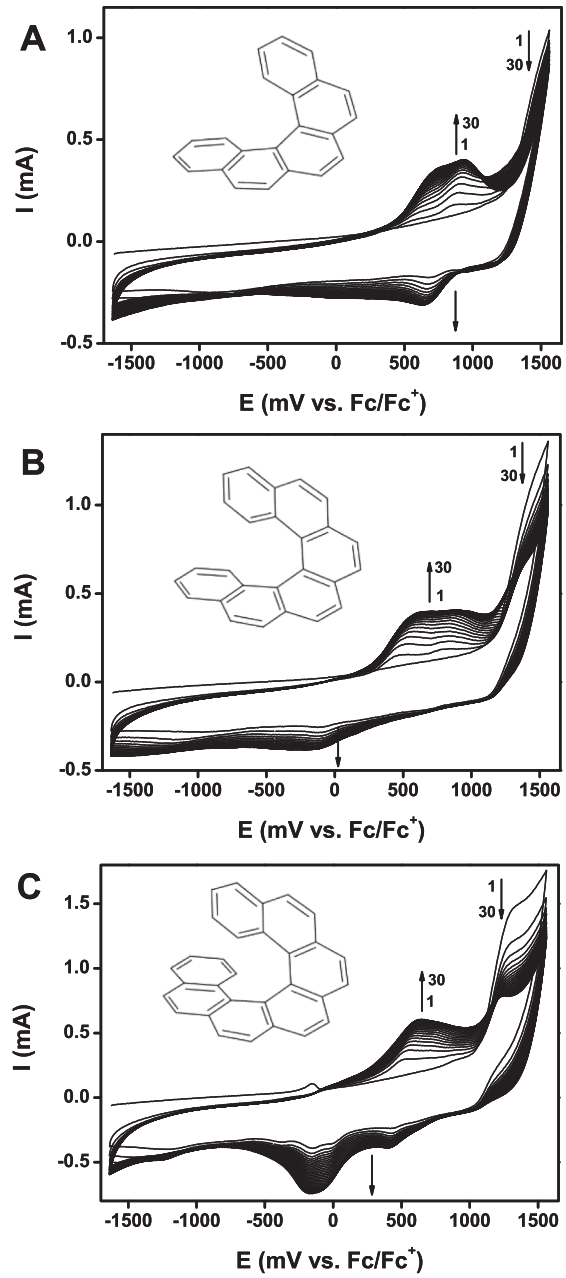

Fig. 1. CV records of 1 mM racemic **(A)** [5]helicene, **(B)** [6]helicene and **(C)** [7]helicene (for structures, see Insets) in deaerated 0.1 M TBAP/ACN electrolyte at GC electrode. The CV scan was finished at the negative potential limit. Scan rate 10 V/s.

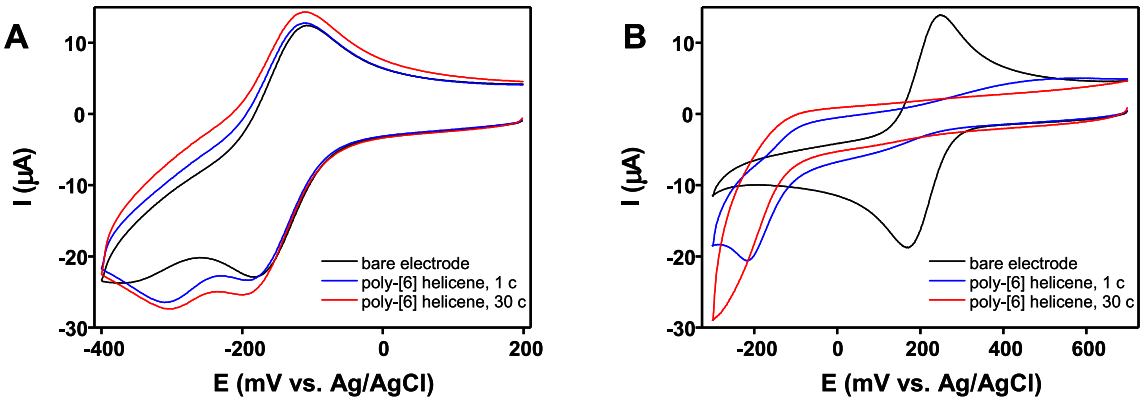

Fig. 2. Cyclic voltammograms of **(A)** hexaammineruthenium(III) and **(B)** hexacyanoferrate (III) redox markers (1 mM) in 0.1 M KCl recorded at bare GC electrode, treated by single CV cycle in 0.1 M TBAP/ACN (black curves), and on GC electrode equipped with [6]helicene layer electrodeposited from 2.5 mM racemic [6] helicene deaerated solution in 0.1 M TBAP/ACN using a single CV cycle (blue curves) or 30 (red curves) CV cycles between −200 and 1800 mV *vs.* Ag pseudo-reference electrode (−638 and 1362 mV *vs.* Fc/Fc+). Scan rate 10 V/s. (For interpretation of the references to colour in this figure legend, the reader is referred to the web version of this article.)

rates (> ca. 5 V·s^{-1}) in the process of potentiodynamic polymerization is most likely caused by the instability of the produced film in the oxidized state. The reduced films withstood transfer from monomer solution, washing and exposure to ambient air during the redox cycling experiments carried out at 10 V·s^{-1} (Fig. S1 in Supporting Information). The same experiments performed with oxidized layers (*i.e.*, those for which the electropolymerization was finished after the +0.8 V peak) gave no redox responses (not shown).

The electrochemical properties of racemic [6]helicene deposits were investigated with $[Fe(CN)_6]^{3-/4-}$ and $[Ru(NH_3)_6]^{3+/2+}$ redox probes according to the known methodology [14]. The results showed that the $Ru^{3+/2+}$ redox process can be observed at both bare and [6]helicene-modified electrode surfaces with comparable reversibility (Fig. 2A). Conversely, the redox transition of $[Fe(CN)_6]^{3-/4-}$ is attenuated at the [6]helicene-modified electrode, and this observation is in agreement with the surface sensitivity of the $[Fe(CN)_6]^{3-/4-}$ redox probe (Fig. 2B). The reason for our focus on [6]helicene is based on the fact that [5]helicene has a low racemization barrier, while higher helicenes have higher demands for synthetic work, chiral separation or purification.

To gain a deeper insight into the conductive properties of the prepared redox-active layers, impedance measurements were conducted on freshly prepared layers deposited onto a GC electrode. The redox-active layer of [6]helicene was prepared under identical conditions to those described in Fig. 1. For comparison, the non-conductive (overoxidized) version of the film was prepared by 5 CV cycles between −640 and 2060 mV *vs.* Fc/Fc$^+$ at 100 mV/s. A control experiment was performed using the uncoated GC. The impedance spectra were recorded directly in the solution used for the electrodepositions, at the respective open circuit potentials (OCP) and with an excitation amplitude of 10 mV. The OCP values were identified as 478 mV for the redox-active and 345 mV for the overoxidized film. The results, expressed as a Bode plot (Fig. S2 in Supporting Information) indicate that the redox-active layer has lower resistance than the overoxidized film (2×10^5 Ω *vs.* 4.4×10^5 Ω, fitting the results between 1000 Hz and 0.1 Hz to a simple RC circuit). The control experiment with an uncoated GC electrode (cycled in the supporting electrolyte without [6]helicene monomer) exhibited much lower resistance (~10^2 Ω, not shown). Moreover, the frequency dependences of the phase shift differ significantly between the two types of polymer layers.

3.2. Experiments with ITO electrode

To investigate the chirality of the prepared layers, depositions of pure P and M enantiomers of [6]helicene onto the surfaces of the ITO electrodes (Fig. 3A) were carried out. Redox cycling was performed under similar conditions as with the GC electrode. 1000 cycles at 10 V·s^{-1} in the potential range of –0.4 V and +1.2 V were applied to fabricate a compact polymer layer. The number of 1000 cycles was chosen to allow the ITO electrode to remain for a sufficiently long time in the potential region in which [6]helicene oxidation occurs, *i.e.*, between ca. 1200 mV *vs.* Fc/Fc$^+$ and the anodic limit. The AFM images showing the topology of the layer surfaces are shown in Fig. 3B and 3C. The deposits are formed as light yellow layers on the ITO surfaces with a profile of up to ca. 100 nm, as previously confirmed by detailed ellipsometric analyses [7]. The deposited layers are significantly less diverse than with bare ITO (Fig. S3 in Supporting Information). Similarly to the results obtained at GC electrodes, it appears that the electrode polarization rate is a very important parameter. Applying lower polarization rates < approx. 1 V·s^{-1}) does not result in redox-active films. The structure and thickness of the layer can be modulated by changing the polarization rate or the time that electrolysis takes place, as has been shown earlier [12,13].

ITO glasses modified with electrodeposited enantiopure [6]helicene-derived layers were subjected to solid-state CD analysis. Fig. 4A shows the CD responses of the films obtained from (*P*)-and (*M*)-[6]helicene as red and blue curves, respectively. To reduce any birefringence or anisotropy effects of the films, we took an average of several spectra, *i.e.* averaged sums from the opposite faces of the film and at different positions of the film. In addition, we measured spectra upon rotating the samples, but no changes were observed. The measurements were performed between 300 and 400 nm, *i.e.* in the region where the samples showed absorption, for details see Fig. S4 in Supporting Information. As expected, the CD spectra showed opposite and strong responses. From Fig. 4A, one can clearly see a positive (negative) CD-active band around 330 nm for the (*P*)-layer ((*M*)-layer). This band exhibits strong ellipticity (between −15 and +26) and may be assigned to the typical π–π* transitions, thanks to its similarly to the band observed at 325 nm in the [6]helicene enantiomers in solution, with a 5-nm red shift, see Ref. [7].

Finally, Raman spectroscopy was used to better characterize the layers electrodeposited on ITO. Raman spectra of ITO slides covered

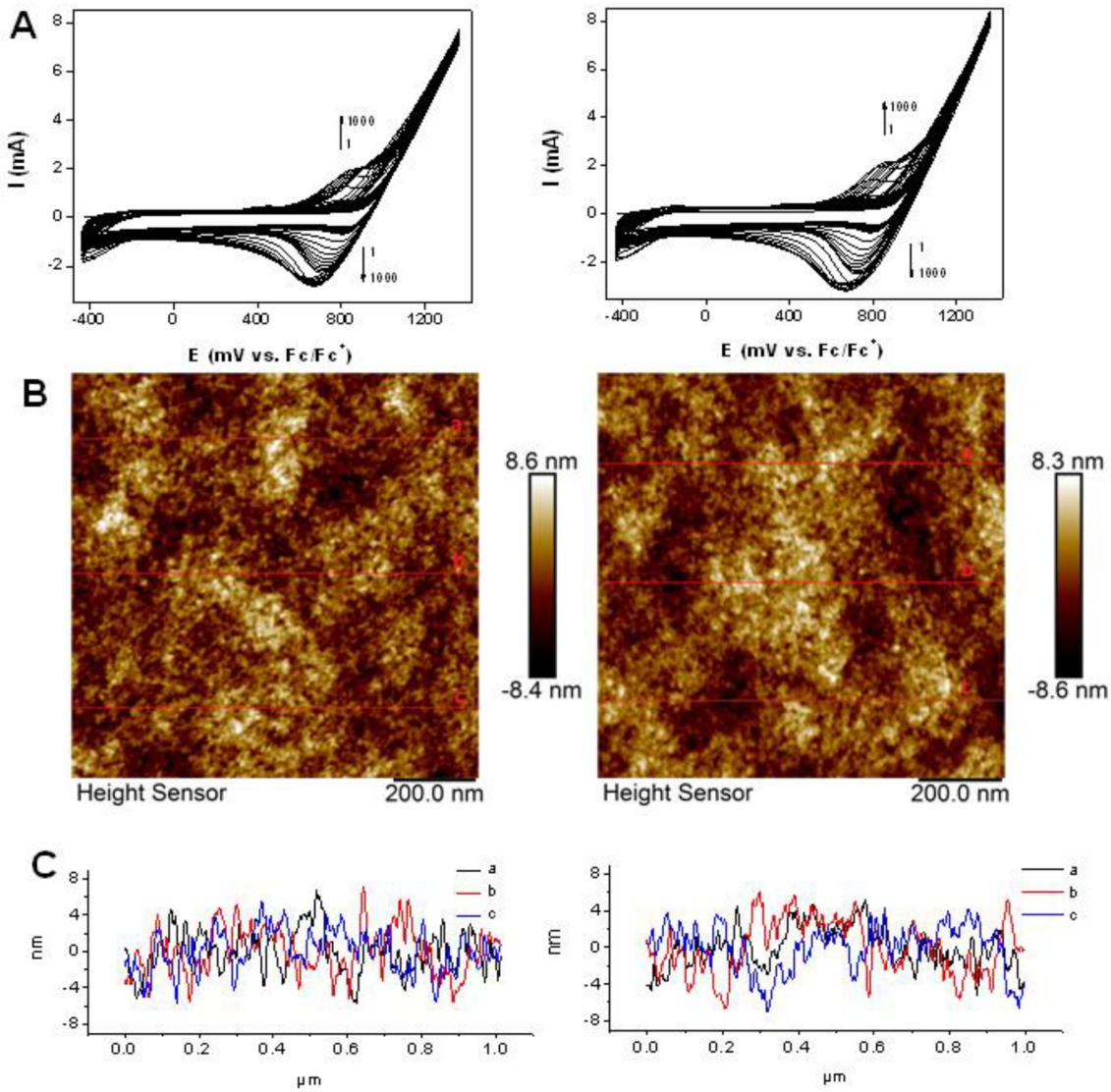

Fig. 3. (A) CV records showing enantiopure [6]helicene layer growth on ITO electrode. Left (*P*-enantiomer), right (*M*-enantiomer), 5 mM [6]helicene monomers were electrodeposited in deaerated 0.1 M TBAP/ACN. Selected CV scans are shown: 1, 2…10th; 20, 30…100th and 200, 300…1000th. Scan rate 10 V/s. Corresponding **(B)** AFM images and **(C)** profilometric analysis of *P*- and *M*-enantiopure [6]helicene films at ITO electrode.

with racemic [6]helicene layers were recorded at a wavelength of 325 nm in the region between 0 and 3300 cm^{-1} (Fig. 4B). For [6]helicene, the most prominent peak in the Raman spectrum is 1359 cm^{-1}, and a group of peaks occurs at around 1600 cm^{-1} [15]. In electropolymerized [6]helicene layers, where [6]helicene units are interconnected, a Raman spectrum similar to carbon nanomaterials is expected. Indeed, the layers deposited onto ITO electrodes exhibit such Raman characteristics, *i.e.* a G band at 1610 cm^{-1} and a D band around 1340 cm^{-1} [14]. In both redox-active and overoxidized layers, the G and D bands are relatively sharp, see Fig. 4B, but superimposed on a broad feature in the spectrum. This is typical for more disordered carbonaceous samples in which the broad feature originates from the combination of several bands spreading over the entire D-G region; peaks D3-D5, see *e.g.* [16,17]. These peaks are often explained as contributions from non-C6 rings. The G and D bands are sharper for the redox-active layer, for which the contribution of the D3-5 bands is also much less. Distinct differences in the Raman patterns of the conductive *vs.* non-conductive version of the [6]helicene layer were also found in the region of secondary Raman peaks (overtones). For the redox-active version of the polymer, the 2D peak at 2691, combination D + D' peak at 2956 and 2D' peak at 3221 cm^{-1} are very well resolved while an unresolved, steeply rising signal is observed in the spectrum of the overoxidized film. It can be concluded that the structure of the redox-active film is more regular than that of the overoxidized version.

4. Conclusions

The chiral resolution phenomenon is now intensively applied in the field of electrochemical research in the form of molecularly imprinted polymers, self-assembled monolayers and chiral metal-based materials [18]. The aim is to develop chiral surfaces or detection platforms that will further be used in the chiral analysis of drugs, in the development of CPL (circularly polarized light) detectors and molecular switches. This communication describes an electrochemical approach suitable for the preparation of nm-thick redox-active layers based on carbohelicenes. The layers were anodically deposited onto the surface of GC and

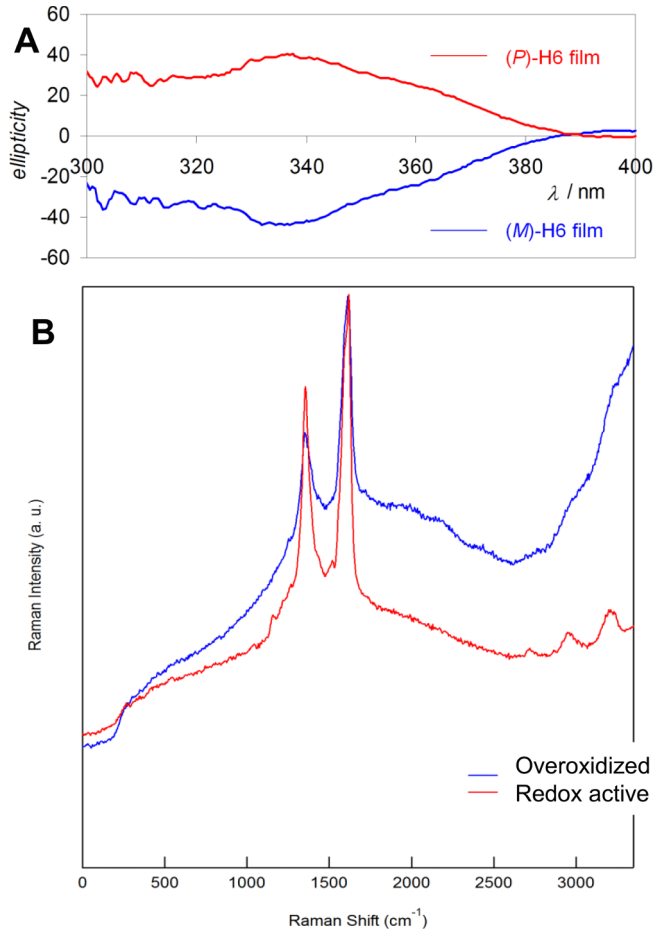

Fig. 4. (A) CD spectra of *P*- and *M*-enantiopure [6]helicene films at ITO electrode. **(B)** Raman spectra of redox-active and overoxidized polymer layers deposited from racemic [6]helicene onto ITO electrode; recorded at 325 nm. For more details, see Fig. 3.

ITO electrodes, and characterized by CD, Raman and impedance spectroscopies and AFM imaging techniques. The results achieved may be the first step in the development and preparation of chiral carbon materials, which may be further applied in materials science, molecular and analytical electrochemistry and spectroelectrochemistry.

Declaration of Competing Interest

The authors declare that they have no known competing financial interests or personal relationships that could have appeared to influence the work reported in this paper.

Acknowledgements

The authors gratefully acknowledge the financial support of RVO 61989592, COST LD 15058 and project LO1409 and SAFMAT LM2015088 from the Ministry of Education, Youth and Sports of the Czech Republic as well as from Masaryk University grant MUNI/A/1359/2018. The study was also partially supported by GACR 16-12757S. We wish to thank Ben Watson-Jones MEng for providing linguistic assistance.

Appendix A. Supplementary data

Supplementary data to this article can be found online at https://doi.org/10.1016/j.elecom.2020.106689.

References

[1] K. Dhbaibi, L. Favereau, J. Crassous, Enantioenriched helicenes and helicenoids containing main-group elements (B, Si, N, P), Chem. Rev. 119 (2019) 8846–8953.
[2] M. Gingras, One hundred years of helicene chemistry. Part 3: Applications and properties of carbohelicenes, Chem. Soc. Rev. 42 (2013) 1051–1095.
[3] M. Gingras, One hundred years of helicene chemistry. Part 1: Non-stereoselective syntheses of carbohelicenes, Chem. Soc. Rev. 42 (2013) 968–1006.
[4] M. Gingras, G. Felix, R. Peresutti, One hundred years of helicene chemistry. Part 2: Stereoselective syntheses and chiral separations of carbohelicenes, Chem. Soc. Rev. 42 (2013) 1007–1050.
[5] C.-F. Chen, Y. Shen, Helicene Chemistry: From Synthesis to Applications. Springer, Heidelberg (2017).
[6] Y. Yang, R.C. da Costa, D.M. Smilgies, A.J. Campbell, M.J. Fuchter, Induction of circularly polarized electroluminescence from an achiral light-emitting polymer via a chiral small-molecule dopant, Adv. Mater. 25 (2013) 2624–2628.
[7] J. Vacek, J. Hrbac, T. Strasak, V. Cirkva, J. Sykora, L. Fekete, J. Pokorny, J. Bulir, M. Hromadova, J. Crassous, J. Storch, Anodic deposition of enantiopure hexahelicene layers, ChemElectroChem 5 (2018) 2080–2088.
[8] Y. Kalachyova, O. Guselnikova, R. Elashnikov, I. Panov, J. Zadny, V. Cirkva, J. Storch, J. Sykora, K. Zaruba, V. Svorcik, O. Lyutakov, Helicene-SPP-based chiral plasmonic hybrid structure: toward direct enantiomers SERS discrimination, ACS Appl. Mater. Interfaces 11 (2019) 1555–1562.
[9] J. Storch, K. Kalikova, E. Tesarova, V. Maier, J. Vacek, Development of separation methods for the chiral resolution of hexahelicenes, J. Chromatogr. A 1476 (2016) 130–134.
[10] J. Hrbac, V. Halouzka, L. Trnkova, J. Vacek, eL-Chem Viewer: a freeware package for the analysis of electroanalytical data and their post-acquisition processing, Sensors 14 (2014) 13943–13954.
[11] S. Arnaboldi, S. Cauteruccio, S. Grecchi, T. Benincori, M. Marcaccio, A.O. Biroli, G. Longhi, E. Licandro, P.R. Mussini, Thiahelicene-based inherently chiral films for enantioselective electroanalysis, Chem. Sci. 10 (2019) 1539–1548.
[12] J. Hrbac, J. Storch, V. Halouzka, V. Cirkva, P. Matejka, J. Vacek, Immobilization of helicene onto carbon substrates through electropolymerization of [7]helicenylthiophene, RSC Adv. 4 (2014) 46102–46105.
[13] J. Hrbac, T. Strasak, L. Fekete, V. Ladanyi, J. Pokorny, J. Bulir, M. Krbal, J. Zadny, J. Storch, J. Vacek, Potential-driven on/off switch strategy for the electrosynthesis of [7]helicene-derived polymers, ChemElectroChem 4 (2017) 3047–3052.
[14] R.L. McCreery, Advanced carbon electrode materials for molecular electrochemistry, Chem. Rev. 108 (2008) 2646–2687.
[15] C. Thomsen, M. Machon, S. Bahrs, Raman spectra and DFT calculations of the vibrational modes of hexahelicene, Solid State Commun. 150 (2010) 628–631.
[16] K. Jurkiewicz, M. Pawlyta, D. Zygadlo, D. Chrobak, S. Duber, R. Wrzalik, A. Ratuszna, A. Burian, Evolution of glassy carbon under heat treatment: correlation structure-mechanical properties, J. Mater. Sci. 53 (2018) 3509–3523.
[17] M. Pawlyta, J.-N. Rouzaud, S. Duber, Raman microspectroscopy characterization of carbon blacks: spectral analysis and structural information, Carbon 84 (2015) 479–490.
[18] D. Mandler, Chiral self-assembled monolayers in electrochemistry, Curr. Opin. Electrochem. 7 (2018) 42–47.